Epilepsy & Behavior Case Reports 5 (2016) 57–65

Contents lists available at ScienceDirect

Epilepsy & Behavior Case Reports

journal homepage: www.elsevier.com/locate/ebcr

Case Report

# Dynamics of epileptic activity in a peculiar case of childhood absence epilepsy and correlation with thalamic levels of GABA

Alberto Leal [a,*], José P. Vieira [b], Ricardo Lopes [c], Rita G. Nunes [d], Sónia I. Gonçalves [e], Fernando Lopes da Silva [f,g], Patrícia Figueiredo [g]

[a] Department of Neurophysiology, Centro Hospitalar Psiquiátrico de Lisboa, Lisbon, Portugal`
[b] Department of Pediatric Neurology, Hospital Dona Estefânia, Lisbon, Portugal
[c] Faculty of Psychology and Educational Sciences, University of Coimbra, Coimbra, Portugal
[d] Instituto de Biofísica e Engenharia Biomédica, Faculdade de Ciências, Universidade de Lisboa, Lisbon, Portugal
[e] Institute of Biomedical Imaging and Life Sciences, Faculty of Medicine, University of Coimbra, Coimbra, Portugal
[f] Center of Neuroscience, Swammerdam Institute for Life Sciences, University of Amsterdam, The Netherlands
[g] Department of Bioengineering and Institute for Systems and Robotics (ISR/IST), LARSyS, Instituto Superior Técnico, Universidade de Lisboa, Portugal

ARTICLE INFO

*Article history:*
Received 13 January 2016
Received in revised form 14 March 2016
Accepted 25 March 2016
Available online 6 April 2016

*Keywords:*
Childhood absence epilepsy
GABA
Thalamus
Human

ABSTRACT

*Objectives:* Childhood absence epilepsy (CAE) is a syndrome with well-defined electroclinical features but unknown pathological basis. An increased thalamic tonic GABA inhibition has recently been discovered on animal models (Cope et al., 2009), but its relevance for human CAE is unproven.
*Methods:* We studied an 11-year-old boy, presenting the typical clinical features of CAE, but spike–wave discharges (SWD) restricted to one hemisphere.
*Results:* High-resolution EEG failed to demonstrate independent contralateral hemisphere epileptic activity. Consistently, simultaneous EEG–fMRI revealed the typical thalamic BOLD activation, associated with caudate and default mode network deactivation, but restricted to the hemisphere with SWD. Cortical BOLD activations were localized on the ipsilateral pars transverse. Magnetic resonance spectroscopy, using MEGA-PRESS, showed that the GABA/creatine ratio was 2.6 times higher in the hemisphere with SWD than in the unaffected one, reflecting a higher GABA concentration. Similar comparisons for the patient's occipital cortex and thalamus of a healthy volunteer yielded asymmetries below 25%.
*Significance:* In a clinical case of CAE with EEG and fMRI-BOLD manifestations restricted to one hemisphere, we found an associated increase in thalamic GABA concentration consistent with a role for this abnormality in human CAE.


## 1. Introduction

Childhood absence epilepsy (CAE) is a well-defined electroclinical syndrome [1], whose neurophysiological markers are generalized bursts of 3-Hz spike–wave discharges (SWD). Since the 50s, several theories have postulated a variable role of the thalamus and neocortex in the genesis of SWD [2]. The most recent twist is the neocortical theory, elaborated from the experimental demonstration of drivers of SWD in specific areas of the cortex in animal genetic models of absence epilepsy [3,4].

In humans, coregistered EEG–functional magnetic resonance imaging (fMRI) has very consistently shown blood oxygen level dependent (BOLD) activation of the thalamus and deactivation of the caudate and default mode network (DMN) [5,6,7]. Cortical BOLD activation areas proved much less consistent and variable among subjects [8]. Slow and delayed neurovascular responses have precluded the construction of a detailed dynamical model of SWD, based on BOLD-fMRI data, especially taking into consideration that the microphysiological animal studies revealed a fast (millisecond scale) propagation of SWD from the initial cortical driving network to other cortical and subcortical areas [3]. In contrast, source analysis methods in EEG [9,10] and MEG [11,12,13] have taken advantage of their high temporal resolution to establish the frontal lobes as the main drivers of SWD.

The underlying causes of the excitability changes in CAE have remained elusive, but a peculiar susceptibility of this condition to antiepileptic drugs promoting γ-aminobutyric acid (GABA) inhibition, such as vigabatrin and tiagabine, suggests that a dysfunction of GABA inhibition in the thalamocortical circuitry might play a role. Because no clear evidence has been found for a synaptic GABA-A or GABA-B dysfunction in a wide range of animal models of CAE [14,15], attention

* Corresponding author at: Avenida do Brasil 53, 1749-002 Lisbon, Portugal.
*E-mail address:* a.leal@neuro.pt (A. Leal).

http://dx.doi.org/10.1016/j.ebcr.2016.03.004

has turned to another locus of action of GABA, the extrasynaptic neuronal receptors responsible for tonic inhibition [16].

This line of research proved fruitful, and in the thalamus, an abnormal increase in tonic GABA-A in animal models of CAE has been found [17], providing a new mechanism for the genesis of SWD in CAE. The relevance of this mechanism for the human condition has not yet been established.

In this paper, we study a peculiar case of CAE with 3-Hz SWD restricted to one hemisphere, therefore, allowing a comparison between this and the contralateral reference hemisphere in the same subject. We explore the unique methodological opportunity this case offers to build an integrated model of EEG and neurovascular responses associated with SWD and to correlate this with thalamic GABA levels across the two hemispheres, as measured by magnetic resonance spectroscopy (MRS).

## 2. Patient data and methods

### 2.1. Clinical data

The patient is an 11-year-old boy, the younger of two sons of healthy and nonconsanguineous parents. The gestational period, delivery, and neonatal period were free of pathologies. He started to walk autonomously around 12 months of age, but the language acquisition was slightly delayed to the age of 3 years. He demonstrated a normal behavior for his age, with good social skills. At the age of 6 years, he started brief episodes of absences, accompanied by staring, motor slowing, chewing, and manual automatisms. These events occurred several times daily and persisted for 4 months, but ceased completely after medication with VPA 500 mg twice daily. The EEG revealed normal background activity, with bursts of high amplitude SWD at 3 Hz, maximum over anterior head electrodes and an odd asymmetry: high amplitude paroxysms were clearly seen over the left hemisphere while they had a smaller amplitude over the right hemisphere (Fig. 1A). No paroxysmal activity was evoked by intermittent photic stimulation, and sleep was well-structured, with symmetrical spindles, vertex waves, and K-complexes (Fig. 1B). School performance fell below average, with particular difficulties in mathematics. At the age of 11 years, the EEGs persistently demonstrate SW discharges, despite the disappearance of clinical seizures. The patient was studied in a program aproved by the ethics commitee of the Centro Hospitalar Psiquiátrico de Lisboa for the study of epilepsy.

### 2.2. Neuropsychological assessment

The neuropsychological assessment at 10 years of age included a global cognitive measure (IQ) and more specific cognitive performance capabilities. The IQ was measured using the Portuguese version of the Wechsler Intelligence Scale for Children (WISC-III). The specific cognitive assessment addressed hemispheric motor dominance, memory, language, attention, executive functions, and motor skills, using the Coimbra Neuropsychological Assessment Battery (CNAB) [18]. This battery has been validated for Portuguese children from age 5 to 15 years, and it has been used clinically in epilepsy studies [19]. The patient was motivated and performed well in the assessment.

### 2.3. Standard EEG recording and processing

The patient was studied with intermittent clinical EEGs using 19 electrodes of the 10–20 system (256-Hz sampling rate), in accordance with common guidelines for pediatric clinical studies, including prolonged hyperventilation, sleep, and photic stimulation. Spectral analysis of EEG signal with a focus on the alpha band was carried out using standard fast Fourier transform (FFT) on a 10-second epoch of wakefulness with eyes closed (Fig. 1C, left), while for spindles, $N = 40$ epochs of 1 s were used (Fig. 1C, right). Additionally, a 2-hour high-resolution EEG recording was performed using 82 scalp electrodes (Fig. 1A). The EEG was evaluated using average and Laplacian montages [20], computed from a realistic scalp surface. Somatic-sensory evoked potentials (SSEP) were obtained through electrical stimulation of the median nerve in the left and right wrists and computed for each hemisphere at C3/4 and CP3/4 (Fig. 1D). Significance of interhemispheric amplitude differences was statistically evaluated in the time window (0 to +100 ms) by using a t-test at each time point. A randomization test with $N = 5000$ permutations was performed.

### 2.4. EEG–fMRI recording and processing

Forty minutes of simultaneous EEG–fMRI data were collected on a whole body 3T system using conventional EPI (TR/TE = 2500/30 ms), and a 32-channel MR-compatible EEG system, during which a single burst of 3-Hz SWD with a duration of 15 s was recorded (Fig. 2A). Magnetization-Prepared Rapid Gradient-Echo (MP-RAGE) images were collected for anatomical reference.

The EEG data were corrected for MR-induced artifacts, and the 15-s burst of 3-Hz SWD was decomposed in independent components (ICs) using EEGLAB [21]. Components with nondipolar fields and time courses compatible with artifacts were visually excluded, yielding 16 remaining ICs (Fig. 3A) [21]. Automatic voltage threshold spike detection of component IC3 was performed, and the detected points were used to segment data in epochs of −50 to 300 ms, centered on the spikes. Segments representing the SWD were then averaged, and the components with larger amplitude were visually classified into spikes (S) and waves (W) (Fig. 3B). Neuronal sources of the S and W were calculated using cortical sLORETA, as implemented in CURRY 6.0 (Compumedics-Neuroscan), and a realistic model for the head derived from the MP-RAGE images, and with electrode positions recovered from surface rendering the recording cap. The temporal dynamics of components was evaluated using the linear cross-correlation r2 and nonlinear h2 metrics [22] allowing the estimation of time-delays between ICs [23].

Functional magnetic resonance imaging data were analyzed using FSL (http://fsl.fmrib.ox.ac.uk), including standard preprocessing and general linear model analysis. Voxels exhibiting significant positive/negative BOLD signal changes that correlated with the 15-s SWD event were identified by cluster thresholding (cluster $p < 0.05$, voxel $z > 2.3$). Freesurfer (http://surfer.nmr.mgh.harvard.edu/) was used for tissue segmentation and cortical reconstruction from MP-RAGE images.

### 2.5. MRS-GABA

γ-Aminobutyric acid spectra were acquired on a whole body 3T system, using a 12-channel head coil, and the sequence MEGA-PRESS [24]. For anatomical reference, T1-weighted MP-RAGE 1-mm$^3$ isotropic resolution images were acquired. Four data sets, with the $25 \times 20 \times 30$-mm$^3$ voxel successively placed on the left (right) thalamus and on the left (right) occipital cortex (Fig. 4) were acquired. Other sequence parameters were as follows: TE/TR = 68/1500 ms, 200 (300) averages acquired with water suppression for occipital cortex (thalamus) and 50 without water suppression, and acquisition time 10 (15) min. Creatine (Cr)

**Fig. 1.** EEG analysis. A) High-resolution EEG (82 electrodes) recording of onset of a 3-Hz SW burst, using average (left) and Laplacian (right) references. Topographic maps of an average spike at peak and half-peak amplitudes are shown. Vertical dotted lines signal 1-s intervals. Vertical scale is 1 mV (left) and 160 μV/cm$^2$ (right). B) EEG sample of phase II sleep, with well-formed and symmetrical spindles. C) Spectra of alpha (left) and spindles (right) for the left and right hemisphere, highlighting the symmetrical features. D) Somatic-sensory evoked potentials to stimulation of the median nerve. The N20 and P25 potentials of each hemisphere to stimulation of the contralateral peripheral nerve are overlapped both for the C3/4 and CP3/4 electrode positions on the scalp. Vertical scale: 2.5 μV, horizontal scale: 20 ms.

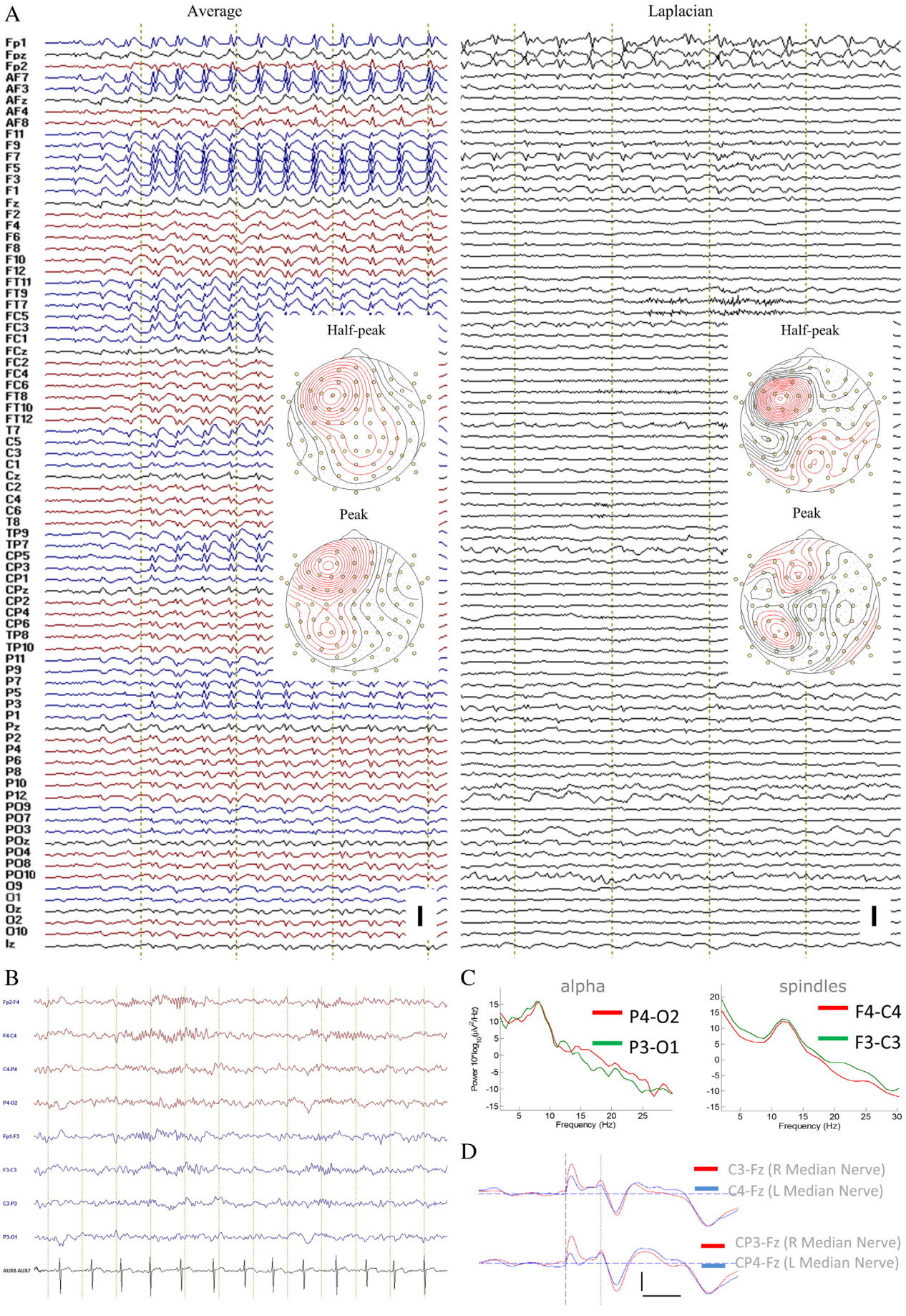
A
Average
Laplacian
Fp1
Fpz
Fp2
AF7
AF3
AFz
AF4
AF8
F11
F9
F7
F5
F3
F1
Fz
F2
F4
F6
F8
F10
F12
FT11
FT9
FT7
FC5
FC3
FC1
FCz
FC2
FC4
FC6
FT8
FT10
FT12
T7
C5
C3
C1
Cz
C2
C4
C6
T8
TP9
TP7
CP5
CP3
CP1
CPz
CP2
CP4
CP6
TP8
TP10
P11
P9
P7
P5
P3
P1
Pz
P2
P4
P6
P8
P10
P12
PO9
PO7
PO3
POz
PO4
PO8
PO10
O9
O1
Oz
O2
O10
Iz
Half-peak
Peak
Half-peak
Peak
B
Fp2-F4
F4-C4
C4-P4
P4-O2
Fp1-F3
F3-C3
C3-P3
P3-O1
AUX8-AUX7
C
alpha
P4-O2
P3-O1
Power 10*log10(uV2/Hz)
Frequency (Hz)
spindles
F4-C4
F3-C3
Frequency (Hz)
D
C3-Fz (R Median Nerve)
C4-Fz (L Median Nerve)
CP3-Fz (R Median Nerve)
CP4-Fz (L Median Nerve)

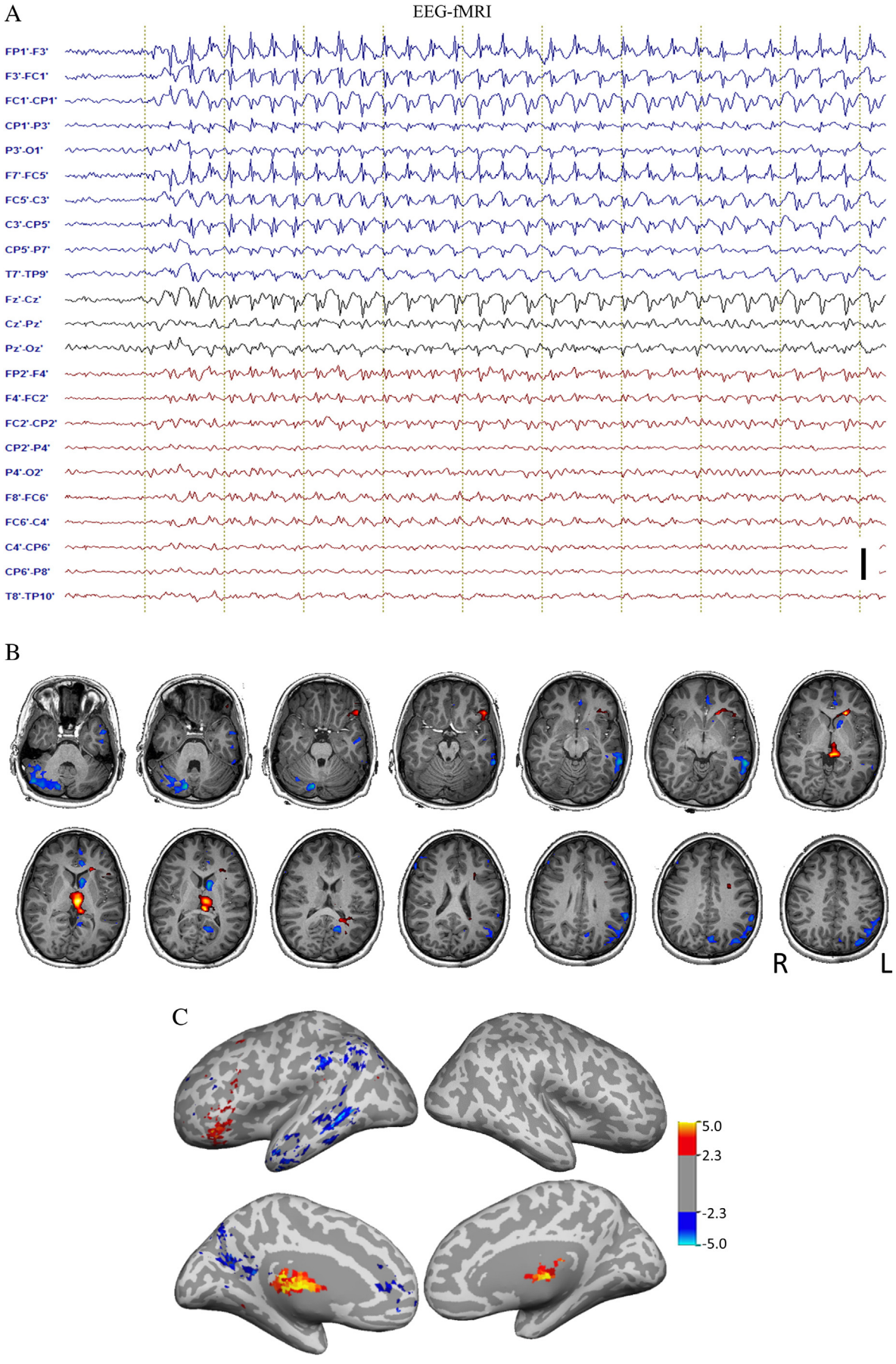
A
EEG-fMRI
FP1'-F3'
F3'-FC1'
FC1'-CP1'
CP1'-P3'
P3'-O1'
F7'-FC5'
FC5'-C3'
C3'-CP5'
CP5'-P7'
T7'-TP9'
Fz'-Cz'
Cz'-Pz'
Pz'-Oz'
FP2'-F4'
F4'-FC2'
FC2'-CP2'
CP2'-P4'
P4'-O2'
F8'-FC6'
FC6'-C4'
C4'-CP6'
CP6'-P8'
T8'-TP10'
B
R
L
C
5.0
2.3
-2.3
-5.0

and water were used as references, and the relative peak areas (GABA/Cr and GABA/water) were determined after spectrum nonlinear fit (Cr and water peaks modeled using Lorentzian shapes, GABA peak assumed to be Gaussian), using Gannet software [25]. The same protocol, but including only thalamic measurements, was applied, as control, to a 29-year-old healthy male volunteer.

## 3. Results

### 3.1. EEG, clinical, and neuropsychological assessments

The background EEG activity was well-preserved, with no abnormalities in alpha, theta, delta, and beta ranges. Sleep was well-structured, with sleep spindles exhibiting normal morphology, abundance, symmetry (Fig. 1B), and spectral features (Fig. 1C). The SSPE had similar amplitudes on both hemispheres (Fig. 1D). These observations failed to demonstrate any asymmetry in physiological spontaneous rhythms and SSEP between hemispheres. Clinical review of the anatomical MRI by a board-certified neuroradiology medical expert, revealed no abnormalities.

The neuropsychological assessment produced a full scale IQ of 103 (verbal IQ: 102 and performance IQ: 105), supporting an average cognitive development. Coimbra Neuropsychological Assessment Battery scores revealed manual left hemisphere dominance, normal memory, language, and executive functions. Isolated abnormalities in the word list and trail making tests supported a minor attention problem.

The high-resolution EEG confirmed the asymmetry of the 3-Hz SWD, with left hemisphere dominance (average reference) and also a trend to higher amplitudes in anterior electrodes (Fig. 1A, left). The Laplacian montage yielded less diffuse changes in spike distribution, but the SWD peaks and phase inversions were restricted to the left hemisphere and midline (Fig. 1A, right), with no clear evidence for a contribution from the right hemisphere.

### 3.2. EEG and BOLD activity

Changes in BOLD signal related to SWD showed activation of the thalamus and frontal lobe pars orbicularis (POr) and pars transverse (PT) areas, while deactivation occurred in the caudate and DMN, all restricted to the left hemisphere (Fig. 2B, C).

The EEG source analysis of SWD-related ICs revealed a distribution of sources over the PT and dorsal frontal lobe of the left hemisphere, while wave-related sources spread over the PT and dorsal and mesial frontal lobes of the same hemisphere (Fig. 3B). Linear correlations between the spike-related components ($h2 = r2$) were found, with consistent time-delay: IC3 leading the other ICs (by 32 ms for IC7 and 20 ms for IC11, with IC11 leading IC7 by 12 ms) (Fig. 3C, left). For wave-related components, a nonlinear contribution was present ($h2 > r2$), with IC2 leading the other ICs (by 40 ms for IC8 and 12 ms for IC10), but the time-delays were less consistent suggesting a more variable pattern of propagation (Fig. 3C, right).

A comparison of BOLD maps with the EEG sources revealed good spatial concordance between the EEG sources and the main positive BOLD cluster (Fig. 3C). The negative BOLD clusters show no spatial colocalization with EEG sources, except at the rostral anterior cingulate (RACi), where the wave-related component IC10 is localized (Fig. 3B, right).

### 3.3. GABA spectroscopy

The GABA-edited NMR spectra for each of the selected voxels are shown in Fig. 4. The position of the voxels on the T1-weighted anatomical image is also shown here. The relative peak areas and the ratios GABA/Cr and GABA/water are shown in Table 1. The results are consistent with a larger GABA concentration in the left thalamus compared with that in the right one (GABA/Cr 2.57 larger, GABA/water 1.61 larger), while only a negligible increase was observed in the concentrations measured in the left versus right occipital cortex (GABA/Cr 1.09 larger and GABA/water 1.01 larger). For the healthy volunteer, the left versus right hemisphere differences were 1.23 larger for GABA/Cr and 0.88 smaller for GABA/water, in the thalamus.

## 4. Discussion

### 4.1. Clinical and EEG data

The analysis of this singular case report puts in evidence the existence of a typical clinical syndrome of CAE, associated with the EEG features and BOLD correlates of such clinical identity, but limited to a single hemisphere. This profound asymmetry is associated with a selective 2.6-fold increase in the GABA/Cr ratio in the affected thalamus, strongly suggesting the involvement of this structure in the expression of the syndrome.

Our patient fulfills established clinical criteria for the diagnosis of CAE [1], regarding age of onset, seizure semiology, high rate of daily seizures, normal cognitive status, and easy pharmacological control of seizures. The EEG background activity was also normal, with apparent interhemispheric symmetry in the alpha rhythm and in cortical excitability (as evaluated by the SSEP). The more detailed study of the sleep spindles also failed to demonstrate asymmetry, which has a special meaning as it does not support the theories interpreting SWD as degenerated spindles [26], suggesting instead that the two phenomena are largely independent despite the involvement of a common thalamus–cortical network [27].

The generalized epilepsy features associated with scalp EEG spike activity restricted to one hemisphere bear resemblance to a group of patients reported by Blume [28] as “hemispheric epilepsy”. He described 13 patients (out of a database of 25,000) with persistently asymmetric EEG spikes associated with generalized ictal features, onset of seizures in childhood, and no demonstrable structural or etiological causes. No cases of CAE were present, and the seizure intractability, multiplicity of seizure types in most patients, as well as frequent secondary bilateral synchronization support the interpretation that our patient does not suffer from this syndrome.

### 4.2. MRS-GABA

The measured left–right interhemispheric proportions of 2.57 and 1.61 in the GABA/Cr and GABA/water ratios of the thalamus are well above what can be explained by the test–retest variability found by Bogner et al. [29] of 0.13 and 0.15, respectively. In contrast, the corresponding ratios in the occipital cortex of the patient (1.09 for GABA/Cr and 1.01 for GABA/water) all fall within the reported test–retest variability. Although these values were reported for the occipital cortex, we believe that our measurements in the thalamus should have comparable quality. In fact, we verified that no significant coil sensitivity differences existed between the two brain regions (occipital cortex and thalamus) in our MRS measurements, and that the shimming was equally good in both regions. In the case of the volunteer, the corresponding ratios (1.25 for GABA/Cr and 0.88 for GABA/water) are higher than expected considering the reported variability, but they are still much lower than that estimated for the patient. A possible explanation for this result is the poorer shim obtained in the volunteer (the width of

**Fig. 2.** EEG–fMRI. A) SW burst during EEG–fMRI recording. Dotted vertical lines are 1-second marks; vertical scale: 500 μV. B) BOLD activation (red) and deactivations (blue) associated with the SW burst, coregistered with the anatomical MRI. C) SW-related BOLD overlaid on the inflated cortical surface. Sulci are represented in deep gray, with corresponding *z*-scores indicated by the color bar.

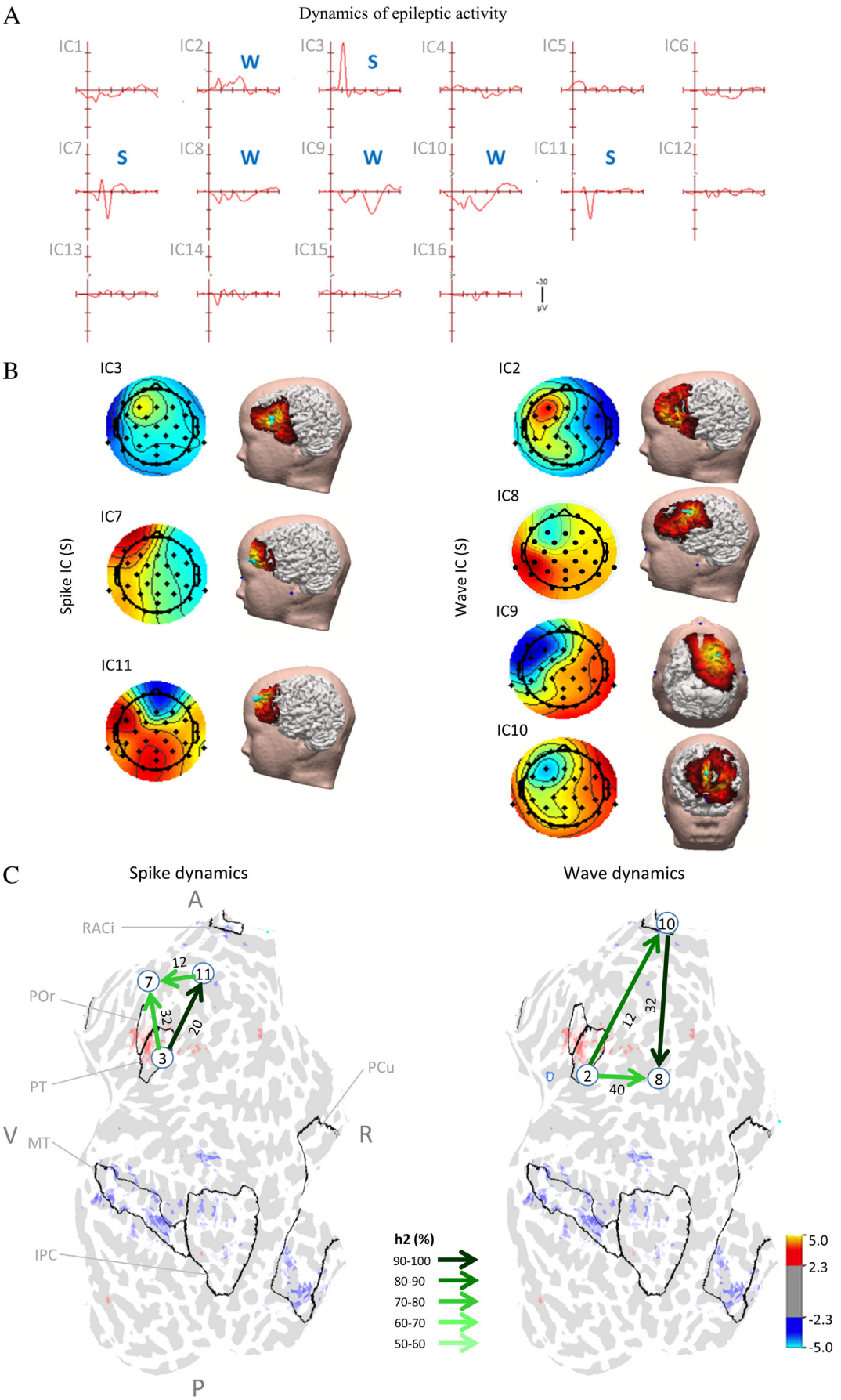
A
Dynamics of epileptic activity
IC1
IC2
W
IC3
S
IC4
IC5
IC6
IC7
S
IC8
W
IC9
W
IC10
W
IC11
S
IC12
IC13
IC14
IC15
IC16
-30
μV
B
IC3
IC7
IC11
Spike IC (S)
IC2
IC8
IC9
IC10
Wave IC (S)
C
Spike dynamics
Wave dynamics
A
RACi
POr
PT
PCu
V
MT
R
IPC
P
7
11
12
22
20
3
10
12
32
2
40
8
h2 (%)
90-100
80-90
70-80
60-70
50-60
5.0
2.3
-2.3
-5.0

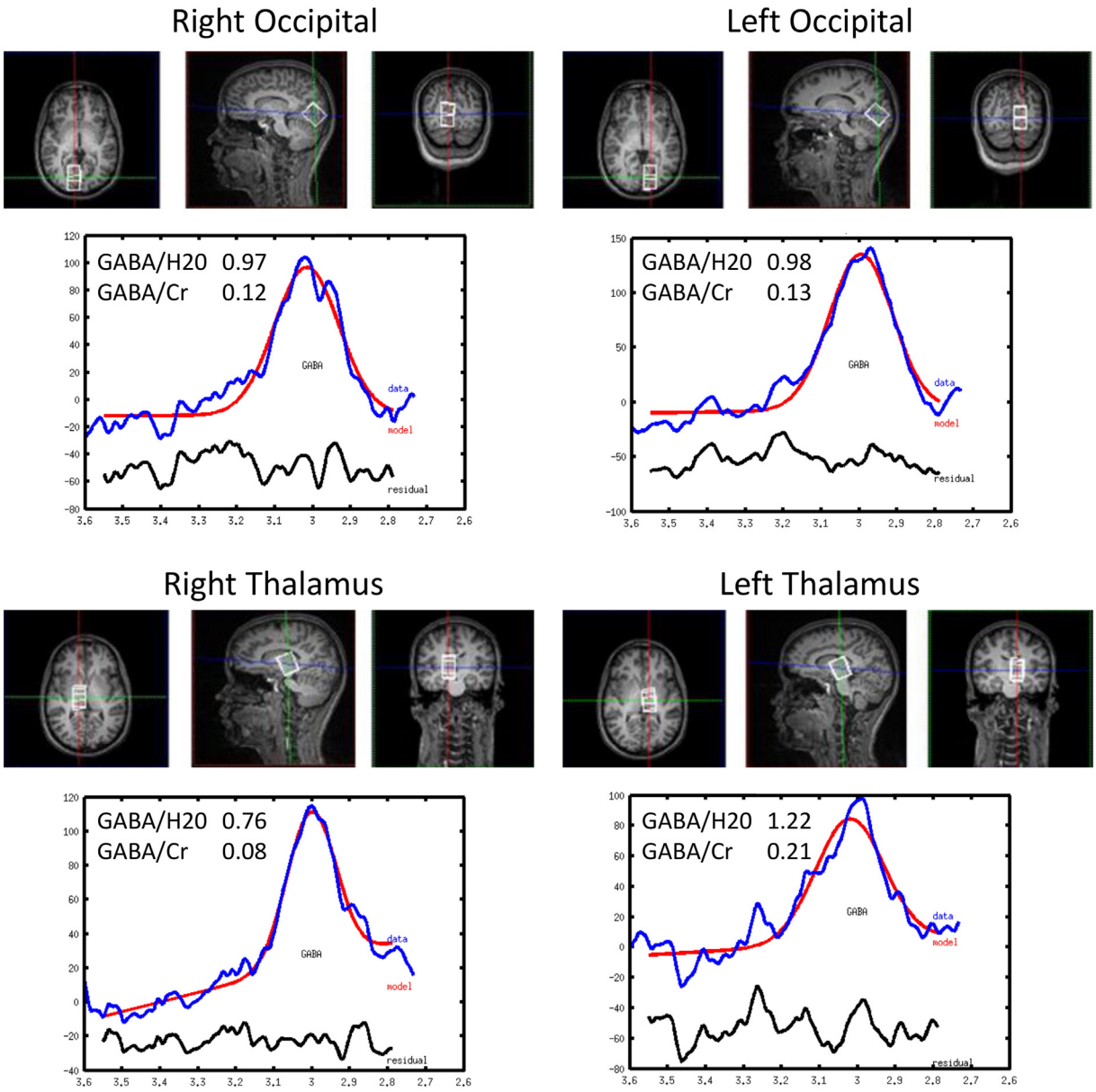


**Fig. 4.** GABA NMR Spectra. Voxel positions for the occipital cortex and thalamus of both hemispheres and corresponding edited GABA spectra for the patient. The estimated areas of the GABA peak relative to the water and Cr reference peaks are shown on the left side of each spectrum. Comparable results were obtained in the two occipital regions with a ratio for the left/right areas of 1.01 (GABA/H20) and 1.09 (GABA/Cr). The thalamic spectra suggest a larger GABA concentration in the left thalamus with ratios of 1.61 (GABA/H20) and 2.57 (GABA/Cr).

the water peak was 22 Hz compared with 15 Hz estimated for the patient).

These results support a true real interhemispheric difference in the GABA concentration of the thalamus of the patient. Rothman et al. [30] found a 2.3-fold increase in the 3.0 ppm GABA/Cr ratio in the occipital lobe of patients with epilepsy medicated with 4.0 g of vigabatrin daily, translating to a calculated 2.9-fold increase in GABA concentration. Furthermore, the comparison with recent determinations of such ratio [31], where a GABA/Cr ratio of 0.071 ± 0.015 was found for a group of 8 healthy volunteers, supports the finding that the right hemisphere GABA/Cr ratio of our patient (0.083) is normal while the left hemisphere ratio (0.213) is pathologically elevated. These values are not likely to be affected by the medication with VPA 1000 mg/day, as Pretoff et al. [32] found no significant effect on GABA brain concentration with VPA doses as high as 1500 mg daily, and more recently, Hattingen et al. [33] also found no reliable differences with VPA therapy, both in the thalamus and motor cortex.

### 4.3. EEG and BOLD data

The patient showed the typical BOLD signature of CAE, with strong thalamic activation and both DMN and caudate deactivations [5,6,7],

**Fig. 3.** Dynamics of average independent components (ICs) resulting from decomposition of the SW recorded during simultaneous EEG–fMRI, classified in spike (S) and wave (W) events. A) IC time courses and classification in spike (S) and wave (W). B) Topographic maps and representation of the sLORETA source analysis results (threshold at 50%) with a dipole at point of maximum score (green), for the spike (left) and wave (right) ICs. C) Correlation analysis, represented in the flattened cortex of the left hemisphere, for the spike (left) and wave (right) IC sources. Arrows point to the direction of lag, and the strength of the association is represented by the color scale. The BOLD scale is in z-score. RACi — rostral anterior cingulate; POr — pars orbicularis; PT — pars transverse; IPC — inferior parietal cortex; MT — medial temporal; PCu — precuneus. Flattened cortex orientation is indicated by P (posterior), V (ventral), R (rostral), and A (anterior).

**Table 1**
Patient GABA NMR spectroscopy results.

| | | GABA/$H_2O$ | GABA/Cr |
|---|---|---|---|
| Occipital | Left | 0.98 | 0.13 |
| | Right | 0.97 | 0.12 |
| | Ratio | 1.01 | 1.09 |
| Thalamus | Left | 1.22 | 0.21 |
| | Right | 0.76 | 0.08 |
| | Ratio | 1.61 | 2.57 |

but limited to the left hemisphere. This observation suggests that the fundamental requirements for SWD are met in the left hemisphere only, particularly in the thalamus. Although the cortical BOLD pattern with POr/PT activation and DMN deactivation has been repeatedly reported in CAE studies, its mechanism remains largely unexplained because of the inherently slow neurovascular response. The EEG analysis of the SWD cortical dynamics in our patient, uncovered a common origin in the PT area, followed by fast spread of spike activity to the dorsal frontal lobe (Fig. 3C, left), while wave-related activity propagated additionally towards the mesial frontal lobe (Fig. 3C, right). Because the spike and wave components of the SWD represent dominant excitatory glutamatergic (spike) and gabaergic (wave) processes [34], these findings indicate that the POr/PT area originated a localized cortical excitation that spread to the dorsal frontal lobe, and a later inhibitory response that spread widely not only to dorsal but also to mesial areas of the frontal lobe. This result for spikes is largely similar to the one of Westmijse et al. [11], who performed source analysis of the magnetoencephalographic 3-Hz SWD, revealing dominant frontal lobe generators in 5 CAE patients. Tenney et al. [13] also found dominant lateral frontal sources using sLORETA in 3-Hz SWD of 12 CAE patients.

The cortical BOLD deactivation areas do not present spatial association with the EEG generators except at the RACi (Fig. 3C, right), which may suggest a special role for this part of the DMN as a region where SW-related gabaergic activity can activate more widespread inhibitory networks.

### *4.4. Increased thalamic GABA can originate childhood absence epilepsy*

The identification of largely increased GABA levels on the left relative to the right thalamus, an asymmetry that was neither present in occipital cortical areas nor in the healthy volunteer, is consistent with the interpretation that this GABA asymmetry may be causally related to the epileptic activity asymmetry. Furthermore, because the increased thalamic GABA occurred in the only hemisphere with SWD, this supports a role in the genesis of this activity and not a simple modification of the usual SWD of CAE. This hypothesis is in line with recent literature demonstrating an important role of the extrasynaptic GABA-induced currents in the control of major thalamocortical rhythms [35] and also that an increase in tonic GABA inhibition plays a fundamental role in SWD in a number of animal models of CAE [14]. Cope et al. [17] have not only demonstrated such abnormality, but also demonstrated that the increase in thalamic tonic GABA inhibition by reverse microdialysis, either of the selective GAT-1 inhibitor NO711 or the extrasynaptic GABA receptor agonist THIP, is sufficient to induce both electrographic and behavioral absence seizures in normal rats. These researchers also demonstrated that knock down of extrasynaptic GABA receptors prevented spontaneous absence seizures in the GAERs model, supporting the interpretation that enhanced extrasynaptic currents are necessary to cause absence seizures.

In accordance with these data, we propose that the increased GABA level that we measured in the left thalamus of our patient is above the threshold for inducing SWD. The observation that no spread of epileptic activity to the contralateral hemisphere occurs, despite the high amplitude and persistence of the left hemisphere SWD, further suggests that the expression of cortical SWD is critically dependent on the interaction with the thalamus expressing a higher concentration of GABA, a condition that is apparently not met in the right hemisphere of our patient.

## Conflict of interest

The authors have no conflict of interest to report.

## Acknowledgments

The authors are grateful to Carla Conceição, MD, for the expert review of the structural MRI and to J. Marques for his help on MRS data acquisition. We acknowledge the Portuguese Science and Technology Foundation (FCT) for financial support through grants PTDC/SAUENB/112294/2009 and UID/EEA/50009/2013. RGN has been funded by the FCT Investigator Program, grant IF/00364/2013.

## References

[1] Hirsch E, Panayiotopoulos C. Childhood absence epilepsy and related syndromes. In: Roger, Bureau, Dravet, Genton, Tassinari, Wolf, editors. Epileptic syndromes in infancy, childhood and adolescence. 4th ed. John Libbey Eurotext Ltd; 2005. p. 315–35.
[2] Avoli M. A brief history on the oscillating roles of thalamus and cortex in absence epilepsy. Epilepsia 2012;53:779–89.
[3] Meeren H, Pijn J, Van Luijtellar E, Coenen A, Lopes da Silva F. Cortical focus drives widespread corticothalamic networks during spontaneous absence seizures in rats. J Neurosci 2002;22:1480–95.
[4] Steriade M. Neuronal substrates of sleep and epilepsy. Cambridge University Press; 2003.
[5] Gotman J, Grova C, Bagshaw A, Kobayashi E, Aghakhani Y, Dubeau F. Generalized epileptic discharges show thalamocortical activation and suspension of the default state of the brain. PNAS 2005;102:15236–40.
[6] Moeller F, Siebner H, Wolff S, Muhle H, Granert O, Jansen O, et al. Simultaneous EEG–fMRI in drug-naïve children with newly diagnosed absence epilepsy. Epilepsia 2008; 49:1510–9.
[7] Bai X, Vestal M, Berman R, Neguishi M, Spann M, Vega C, et al. Dynamic time course of typical childhood absence seizures: EEG, behavior, and functional magnetic resonance imaging. J Neurosci 2010;30:5884–93.
[8] Moeller F, LeVan P, Muhle H, Stephani U, Dubeau F, Siniatchkin M, et al. Absence seizures: individual patterns revealed by EEG–fMRI. Epilepsia 2010;51:2000–10.
[9] Holmes M, Brown M, Tucker D. Are "generalized" seizures truly generalized? Evidence of localized mesial frontal and frontopolar discharges in absence. Epilepsia 2004;45:1568–79.
[10] Moeller F, Muthuraman M, Stephani U, Deuschl G, Raethjen J, Siniatchkin M. Representation and propagation of epileptic activity in absences and generalized photoparoxysmal responses. Hum Brain Mapp 2013;34:1896–909.
[11] Westmijse I, Ossenblock P, Gunning B, van Luijtelaar G. Onset and propagation of spike and slow wave discharges in human absence epilepsy: a MEG study. Epilepsia 2009;50:2538–48.
[12] Gupta D, Ossenblok P, van Luijtelaar G. Space–time network connectivity and cortical activations preceding spike wave discharges in human absence epilepsy: a MEG study. Med Biol Eng Comput 2011;49:555–65.
[13] Tenney J, Fujiwarw H, Horn P, Jacobson S, Glauser T, Rose D. Focal corticothalamic sources during generalized absence seizures: a MEG study. Epilepsy Res 2013;106: 113–22.
[14] Crunelli V, Leresche N, Cope D. $GABA_A$ receptor function in typical absence epilepsy. In: Noebels, Avoli, Rogawski, Olsen, Delgado-Escueta, editors. Jasper's basic mechanisms of the epilepsies. Oxford Press; 2012. p. 228–41.
[15] Han H, Cortez M, Carter Snead IIIO. $GABA_B$ receptor and absence epilepsy. In: Noebels, Avoli, Rogawski, Olsen, Delgado-Escueta, editors. Jasper's basic mechanisms of the epilepsies. Oxford Press; 2012. p. 242–56.
[16] Glykys J, Mody I. Activation of GABA-A receptors: views from outside the synaptic cleft. Neuron 2007;56:763–70.
[17] Cope D, Giovanni G, Fyson S, Orbán G, Errington A, Lorincz M. Enhanced tonic $GABA_A$ inhibition in typical absence epilepsy. Nat Med 2009;15:1392–9.
[18] Simões MR, Albuquerque C, Pinho M, Pereira M, Seabra-Santos M, Alberto I. Coimbra neuropsychological assessment battery — CNAB. Bateria de Avaliação Neuropsicológica de Coimbra (BANC). Lisboa: Cegoc; 2015 [in press]. [(Portuguese)].
[19] Lopes R, Simões M, Leal A. Neuropsychological abnormalities in children with the Panayiotopoulos syndrome point to parietal lobe dysfunction. Epilepsy Behav 2014;31:50–5.
[20] Deng S, Winter W, Thorpe S, Srinivasan R. Improved surface Laplacian estimates of cortical potential using realistic models of head geometry. IEEE Trans Biomed Eng 2012;59:2979–85.
[21] Delorme A, Palmer J, Onton J, Oostenveld R, Makeig S. Independent EEG sources are dipolar. PLoS One 2012;7, e30135.
[22] Pijn J, Vijn P, Lopes da Silva F, Boas W, Blanes W. The use of signal-analysis for the localization of an epileptogenic focus: a new approach. Adv Epileptol 1989;17: 272–6.

[23] Lopes da Silva F. EEG and MEG: relevance to neuroscience. Neuron 2013;80: 1112–28.
[24] Mullins P, McGonigle D, O'Gorman R, Puts N, Vidyasagar R, Evans C. Current practice in the use of MEGA-PRESS spectroscopy for the detection of GABA. Neuroimage 2014;86:43–52.
[25] Edden R, Puts N, Harris A, Barker P, Evans C. Gannet: a batch-processing tool for the quantitative analysis of gamma-aminobutyric acid–edited MR spectroscopy spectra. J Magn Reson Imaging 2014;40:1445–52.
[26] Gloor P. Generalized cortico-reticular epilepsies. Some considerations on the pathophysiology of generalized bilaterally synchronous spike and wave discharge. Epilepsia 1968;9:249–63.
[27] Leresche N, Lambert R, Errington A, Crunelli V. From sleep spindles of natural sleep to spike and wave discharges of typical absence seizures: is the hypothesis still valid? Eur J Physiol 2012;463:201–12.
[28] Blume W. Hemispheric epilepsy. Brain 1998;121:1937–49.
[29] Bogner W, Gruber S, Doelken M, Stadlbauer A, Ganslandt O, Boettcher U, et al. In vivo quantification of intracerebral GABA by single-voxel 1H-MRS — how reproducible are the results? Eur J Radiol 2010;73:526–31.
[30] Rothman D, Petroff O, Behar K, Mattson R. Localized 1H NMR measurements of γ-aminobutyric acid in human brain in vivo. Proc Natl Acad Sci U S A 1993;90:5662–6.
[31] Pan J, Duckrow R, Spencer D, Avdievich N, Hetherington H. Selective homonuclear polarization transfer for spectroscopic imaging of GABA at 7T. Magn Reson Med 2013;69:310–6.
[32] Petroff O, Rothman D, Behar K, Hyder F, Mattson R. Effects of valproate and other antiepileptic drugs on brain glutamate, glutamine and GABA in patients with refractory complex partial seizures. Seizure 1999;8:120–7.
[33] Hattingen E, Luckerath C, Pellikan S, Vronski D, Roth C, Knake S, et al. Frontal and thalamic changes of GABA concentration indicate dysfunction of thalamofrontal networks in juvenile myoclonic epilepsy. Epilepsia 2014;55:1030–7.
[34] Chipaux M, Charpier S, Polack P. Chloride-mediated inhibition of the ictogenic neurons initiating genetically-determined absence seizures. Neuroscience 2011;192: 642–51.
[35] Rovó Z, Mátyás F, Barthó P, Slézia A, Lecci S, Pellegrini C, et al. Phasic, nonsynaptic GABA-A receptor-mediated inhibition entrains thalamocortical oscillations. J Neurosci 2014;34(21):7137–47.